Stem Cell Research 67 (2023) 103038

Contents lists available at ScienceDirect

Stem Cell Research

journal homepage: www.elsevier.com/locate/scr

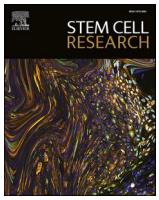

Lab Resource: Genetically-Modified Single Cell Line

# Generation of a ST3GAL3 null mutant induced pluripotent stem cell (iPSC) line (UKWMPi002-A-3) by CRISPR/Cas9 genome editing

David Diouf [a,*], Maria Rosaria Vitale [a], Johanna Eva Maria Zöller [a], Ana-Magdalena Pineau [a], Eva Klopocki [b], Catharina Hamann [a], Georg Christoph Ziegler [a,c], Tim Vanmierlo [d,e], Daniel Van den Hove [d], Klaus-Peter Lesch [a,d,*]

[a] Division of Molecular Psychiatry, Center of Mental Health, University Hospital Würzburg, Würzburg, Germany
[b] Institute of Human Genetics, Biocentre, University of Würzburg, Würzburg, Germany
[c] Department of Psychiatry, Psychosomatics and Psychotherapy, Center of Mental Health, University Hospital Würzburg, Würzburg, Germany
[d] Department of Psychiatry and Neuropsychology, School for Mental Health and Neuroscience (MHeNs), Maastricht University, Maastricht, the Netherlands
[e] Neuro-immune Connect and Repair Lab, Biomedical Research Institute, Hasselt University, Hasselt, Belgium

A B S T R A C T

Fibroblasts isolated from a skin biopsy of a healthy individual were infected with Sendai virus containing the Yamanaka factors to produce transgene-free human induced pluripotent stem cells (iPSCs). CRISPR/Cas9 was used to generate an isogenic cell line carrying an inactivation of *ST3GAL3*, a risk gene associated with neurodevelopmental and psychiatric disorders. This *ST3GAL3* null mutant (*ST3GAL3*-/-) iPSC line, which displays the expression of pluripotency-associated markers, the ability to differentiate into cells of the three germ layers *in vitro*, and a normal karyotype, is a powerful tool to investigate the impact of deficient sialylation of glycoproteins in neural development and plasticity.

## 1. Resource table

| | |
|---|---|
| Unique stem cell line identifier | UKWMPi002-A-3 |
| Alternative name(s) of stem cell line | *ST3GAL3*+/+ (UKWMPi002-A)<br>*ST3GAL3*-/- (UKWMPi002-A-3) |
| Institution | Division of Molecular Psychiatry, Center of Mental Health, University Hospital Würzburg, Würzburg, Germany |
| Contact information of the reported cell line distributor | Klaus-Peter Lesch, kplesch@mail.uni-wuerzburg.de |
| Type of cell line | iPSC |
| Origin | Human |
| Additional origin info *(applicable for human ESC or iPSC)* | Age: 46<br>Sex: Female |
| Cell Source | Dermal fibroblasts |
| Method of reprogramming | Non integrative Sendai Virus |
| Clonality | Clonal |
| Evidence of the reprogramming transgene loss (including genomic copy if applicable) | qRT-PCR |
| Cell culture system used | Matrigel |
| Type of Genetic Modification | Induced deletions |
| Associated disease | Non-syndromic autosomal recessive intellectual disability (NSARID), early infantile epilepsy (EIEE15); attention-deficit/hyperactivity disorder (ADHD) |
| Gene/locus | Gene: *ST3GAL3*; Chr1p34.1; Entrez Gene ID: 6487<br>*ST3GAL3*+/+: NG_028196.1<br>*ST3GAL3*-/-: NM_174963.5: [c.278_288del]; [c. 276_288del] |
| Method of modification/site-specific nuclease used | Streptococcus Pyogenes-CRISPR/Cas9 |
| Site-specific nuclease (SSN) delivery method | Plasmid transfection |
| All genetic material introduced into the cells | pSpCas9(BB)-2A-Puro plasmid vector V2.0 (PX459; Addgene #62988) |
| Analysis of the nuclease-targeted allele status | Sequencing of the targeted allele |
| Method of the off-target nuclease activity surveillance | Targeted PCR/sequencing |
| Name of transgene | N/A |
| Eukaryotic selective agent resistance (including inducible/gene expressing cell-specific) | N/A |
| Inducible/constitutive system details | N/A |
| Date archived/stock date | 11.04.2022 |

(continued on next column)
(continued)
(continued on next page)

* Corresponding authors at: Division of Molecular Psychiatry, Center of Mental Health, University Hospital Würzburg, Margarete-Höppel-Platz 1, 97080 Würzburg, Germany.
*E-mail addresses:* Diouf_D@ukw.de (D. Diouf), kplesch@mail.uni-wuerzburg.de (K.-P. Lesch).

https://doi.org/10.1016/j.scr.2023.103038
Received 14 December 2022; Received in revised form 13 January 2023; Accepted 29 January 2023
Available online 31 January 2023

**Table 1**
Characterization and validation.

| Classification (optional *italicized*) | Test | Result | Data |
|---|---|---|---|
| Morphology | Photography; Bright field microscopy | Cells present typical primed pluripotent human stem cell morphology characteristics: Round, Large nucleus, scant cytoplasm, and sharp edges | Bright-field image; Fig. 1G |
| Pluripotency status evidence for the described cell line | Qualitative analysis (Immunocytochemistry) | Positive expression of the pluripotency associated markers TRA1-60, OCT-3/4, and SSEA-4 | Fig. 1E |
| | Quantitative analysis (qRT-PCR) | Positive relative expression of the pluripotency-related genes: *NANOG*, *REX1*, and *OCT-3/4* | Fig. 1D |
| Karyotype | Karyotype (G-banding) | 46XX, Resolution 450 bands.<br>Cell lines did not present evident chromosomal abnormalities | Fig. 1H |
| Genotyping for the desired genomic alteration/allelic status of the gene of interest | PCR + sequencing | *ST3GAL3*+/+: NG_028196.1<br>*ST3GAL3*-/-: NM_174963.5 [278_288delACACTTACTCC];<br>[276_288delCTACACTTACTCC] | PCR, sequencing: Fig. 1B (Sanger seq track in Suppl. data);<br>cDNA-PCR Fig. 1C (Sanger seq track in Suppl. data) |
| | Transgene-specific PCR | N/A | |
| Verification of the absence of random plasmid integration events | PCR | PCR detection specific for the delivered plasmid backbone | Suppl. Fig. S1B |
| Parental and modified cell line genetic identity evidence | STR analysis | DNA profiles determined by PCR single-locus technology<br>16 independent PCR-systems D8S1179, D21S11, D7S820, CSF1PO, D3S1358, TH01, D13S317, D16S539, D2S1338, AMEL, D5S818, FGA, D19S433, vWA, TPOX and D18S51 were investigated.<br>All loci matched between the two cell lines. | Suppl. Data 2, submitted in the archive with journal |
| Mutagenesis / genetic modification outcome analysis | Sequencing (genomic DNA PCR) | *ST3GAL3*+/+: NG_028196.1<br>*ST3GAL3*-/-: NM_174963.5 [278_288delACACTTACTCC];<br>[276_288delCTACACTTACTCC] | Fig. 1B<br>Sanger seq tracks provided in Suppl. data |
| | PCR-based analyses | *ST3GAL3*-/- lacks an intact gene able to express ST3GAL3 | Fig. 1C |
| | mRNA-PCR and sequencing | *ST3GAL3*-/-, reflecting their genomic state, transcripts present non-sense deletions, leading to frame shifts and the encoding of short non-functional peptides | Suppl. Fig. S3 |
| *Off-target nuclease analysis-* | PCR and sequencing across top 5 predicted likely off-target sites | Most likely off-target (gRNA mismatches):<br>NC_000011.10 [95218059]<br>NC_000010.11 [57394875]<br>NG_016419 [11933782]<br>NC_000005.10 [157315068]<br>NC_000004.12 [158671644]<br>All checked potential off-targets revealed unmodified | Suppl. Fig. S2 |
| Specific pathogen-free status | Mycoplasma | LookOut® Mycoplasma PCR Detection Kit: negative | Suppl. Fig. S1C |
| Multilineage differentiation potential | Directed differentiation | Cells successfully differentiated into all three germ layers with expression of the germ layers-specific markers: FOXA2, CD-144, and PAX-6 | Fig. 1F |
| *Donor screening (OPTIONAL)* | HIV 1, Hepatitis B, Hepatitis C | Negative | not shown but available from corresp. author |
| *Genotype - additional histocompatibility info (OPTIONAL)* | Blood group genotyping | N/A | |
| | HLA tissue typing | N/A | |

(*continued*)

| | |
|---|---|
| Cell line repository/bank | https://hpscreg.eu/cell-line/UKWMPi002-A-3 |
| Ethical/GMO work approvals | Ethics Committee, Medical Faculty, University Hospital Würzburg, 96/11 |
| Addgene/public access repository recombinant DNA sources' disclaimers (if applicable) | N/A |

## 2. Resource utility

Loss-of-function mutations in *ST3GAL3* cause autosomal recessive intellectual disability and infantile epilepsy (Hu et al., 2011; Indellicato et al., 2020). Additionally, *ST3GAL3* has been implicated in genome-wide association studies (GWAS) meta-analyses, particularly on cognition, and ADHD (Demontis et al., 2019). Investigations in an iPSC line carrying a knockout of *ST3GAL3* will elucidate the role of ST3GAL3 in neurodevelopment.

## 3. Resource details

CMP-N-acetylneuraminate-beta-1,4-galactoside-alpha-2,3-sialyl-transferase-III (ST3GAL3) is a type-II membrane protein that catalyzes the transfer of sialic acid to nascent oligosaccharides (Rivero et al., 2021; Schnaar et al., 2014). Several studies have highlighted the crucial roles of ST3GAL3 in brain development and plasticity. Loss-of-function mutations in the gene encoding ST3GAL3 lead to the development of non-syndromic autosomal recessive intellectual disability (NSARID) and early infantile epilepsy (EIEE15) (Hu et al., 2011; Indellicato et al., 2020). Interestingly, these patients do not show clinical features other than neurological symptoms, indicating peripheral compensation but indispensable activity in the brain. Moreover, recent GWAS meta-analyses have linked genetic variation in *ST3GAL3* to a considerable number of phenotypes, including cognition, educational attainment, childhood aggression, and attention-deficit/hyperactivity disorder (ADHD) (Demontis et al., 2019). ST3GAL3 modifies neuronal-cell-adhesion molecule-1 (NCAM1) and cell-adhesion molecule 1 (CADM1/SynCAM1) (Rivero et al., 2021).

Therefore we developed a human iPSC-based *in vitro* model of

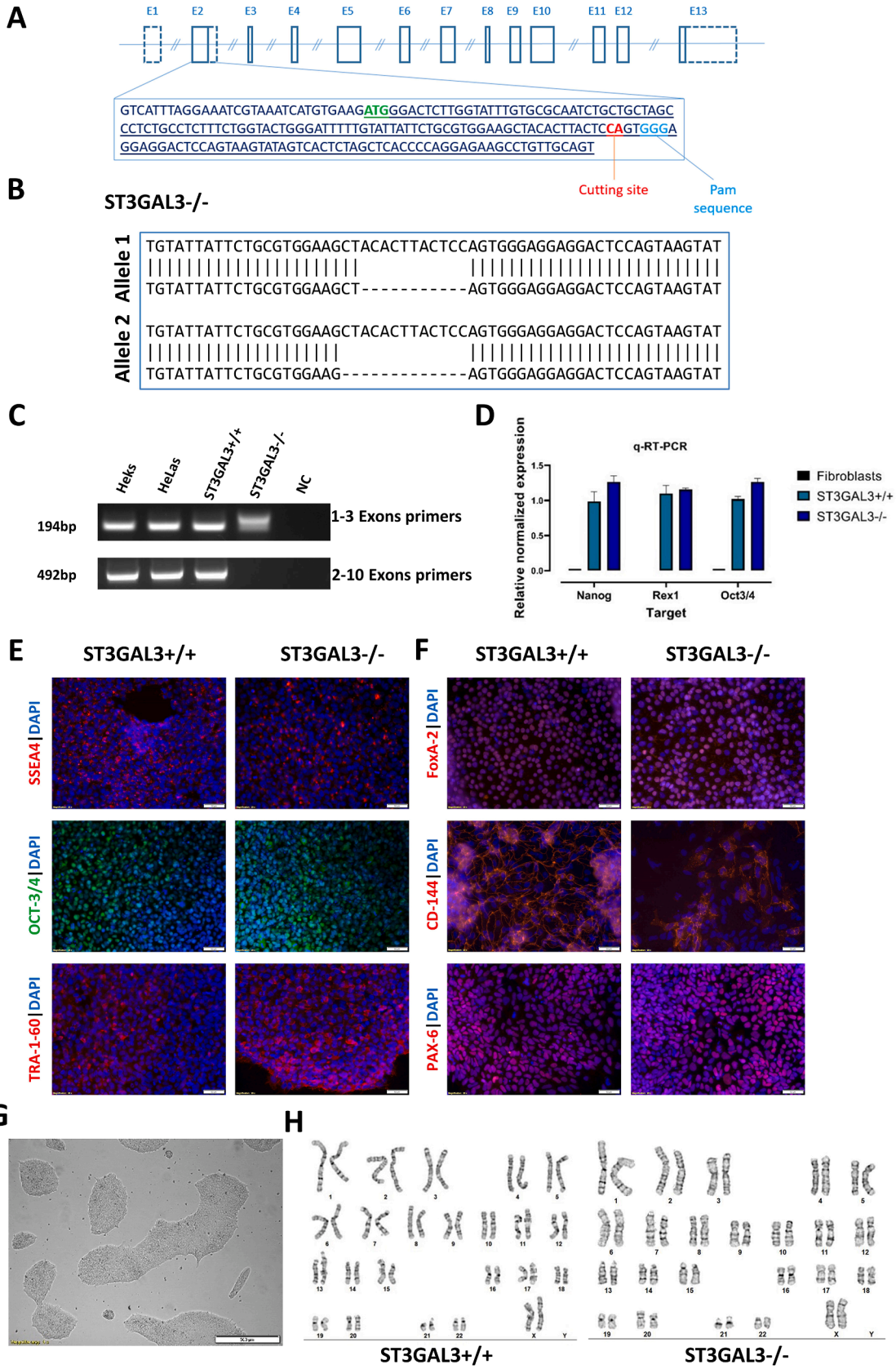
A
E1 E2 E3 E4 E5 E6 E7 E8 E9 E10 E11 E12 E13
GTCATTTAGGAAATCGTAAATCATGTGAAGATGGGACTCTTGGTATTTGTGCGCAATCTGCTGCTAGC
CCTCTGCCTCTTTCTGGTACTGGGATTTTTGTATTATTCTGCGTGGAAGCTACACTTACTCCAGTGGGA
GGAGGACTCCAGTAAGTATAGTCACTCTAGCTCACCCCAGGAGAAGCCTGTTGCAGT
Cutting site
Pam sequence
B
ST3GAL3-/-
Allele 1
TGTATTATTCTGCGTGGAAGCTACACTTACTCCAGTGGGAGGAGGACTCCAGTAAGTAT
TGTATTATTCTGCGTGGAAGCT----------AGTGGGAGGAGGACTCCAGTAAGTAT
Allele 2
TGTATTATTCTGCGTGGAAGCTACACTTACTCCAGTGGGAGGAGGACTCCAGTAAGTAT
TGTATTATTCTGCGTGGAAG----------AGTGGGAGGAGGACTCCAGTAAGTAT
C
Heks
HeLas
ST3GAL3+/+
ST3GAL3-/-
NC
194bp
1-3 Exons primers
492bp
2-10 Exons primers
D
q-RT-PCR
Relative normalized expression
1.5
1.0
0.5
0.0
Nanog
Rex1
Oct3/4
Target
Fibroblasts
ST3GAL3+/+
ST3GAL3-/-
E
ST3GAL3+/+
ST3GAL3-/-
SSEA4|DAPI
OCT-3/4|DAPI
TRA-1-60|DAPI
F
ST3GAL3+/+
ST3GAL3-/-
FoxA-2|DAPI
CD-144|DAPI
PAX-6|DAPI
G
H
ST3GAL3+/+
ST3GAL3-/-

**Fig. 1.**

**Table 2**
Reagents details.

| Antibodies and stains used for immunocytochemistry/flow-cytometry | | | |
|---|---|---|---|
| | Antibody | Dilution | Company Cat # and RRID |
| Pluripotency markers | Mouse anti-OCT-3/4 | 1:50 | Santa Cruz Biotechnology, Cat# sc-5279, RRID: AB_628051 |
| | Mouse anti-SSEA-4 | 1:200 | ThermoFisher Scientific, Cat# MA1-021 RRID: AB_2536687 |
| | Mouse anti-TRA1-60 | 1:50 | Santa Cruz Biotechnology, Cat# sc-21705 RRID: AB_628385 |
| Differentiation markers | Mouse anti-FOXA2 | 1:250 | Santa Cruz Biotechnology, Cat# sc-374376, RRID: AB_10989742 |
| | Rabbit anti-CD-144 | 1:100 | ThermoFisher Scientific, Cat# MA5-32409, RRID: AB_2809687 |
| | Goat anti-PAX6 | 1:100 | R and D Systems, Cat# AF938, RRID: AB_355726 |
| Secondary antibodies | Donkey anti-mouse-555 | 1:1000 | ThermoFisher Scientific, Cat# A-31570, RRID: AB_2536180 |
| | Donkey anti-mouse-488 | 1:1000 | ThermoFisher Scientific, Cat# A-21202, RRID: AB_141607 |
| | Donkey anti-rabbit-488 | 1:1000 | ThermoFisher Scientific, Cat# A-21206, RRID: AB_2535792 |
| | Donkey anti-goat-488 | 1:1000 | ThermoFisher Scientific, Cat# A32814, RRID: AB_2762838 |
| Nuclear stain | DAPI | 1:1000 | ThermoFisher Scientific, Cat# D1306 |
| Site-specific nuclease | | | |
| Nuclease information | S. pyogenes Cas9 | | |
| Delivery method | Plasmid | | |
| Selection/enrichment strategy | Puromycin selection | | |
| Primers and oligonucleotides used in this study | | | |
| | **Target** | **Forward/reverse primer (5′-3′)** | |
| Sendai virus detection | IPSC-SeV | GGATCACTAGGTGATATCGAGC/ ACCAGACAAGAGTTTAAGAGATATGTATC | |
| | IPSC-KOS | ATGCACCGCTACGACGTGAGCGC/ ACCTTGACAATCCTGATGTGG | |
| | IPSC-Klf4 | TTCCTGCATGCCAGAGGAGCCC/AATGTATCGAAGGTGCTCAA | |
| | IPSC-Myc | TAACTGACTAGCAGGCTTGTCG/ TCCACATACAGTCCTGGATGATGAT | |
| Pluripotency markers (qRT-PCR) | NanoG | CTGAGATGCCTCACACGGAG/TGTTTGCCTTTGGGACTGGT | |
| | Rex-1 | AGGTGGCATTGGAAATAGCAGA/AGTGGGGTGGGTTTGCCTA | |
| | Oct-3/4 | CCCACACTGCAGCAGATCA/TGTGCATAGTCGCTGCTTGA | |
| House-keeping genes (qRT-PCR) | *HPRT-1* | CTTGGTCAGGCAGTATAATCCAA/ CTTATAQTCCAACACTTCGTGGGG | |
| | *UBC* | Qiagen (Cat# QT00234430) | |
| | *TBP1* | Qiagen (Cat# QT00000721) | |
| | *GUSB* | Qiagen (Cat# QT00046046) | |
| Genotyping (desired allele/transgene presence detection) | *ST3GAL3* Exon 2 | TGAGATGGGGATGAGCAGG/ AAGGAACTGAGATTTGTCATGGC | |
| Targeted mutation analysis/sequencing | *ST3GAL3* Exon 2 | TGAGATGGGGATGAGCAGG/ AAGGAACTGAGATTTGTCATGGC | |
| | NM_006279.5 | TTATTCTGCGTGGAAGCTACA/TTCAGTCTCACCACAATGTCA | |
| | NM_174963.5 | CCTCTCCGCTGTGGTCATTT/GTCCAGCGGAGTCAAAGGAA | |
| Potential random integration-detecting PCRs | pSpCas9 plasmid backbone detection | GTGAAAGTGATGGGCCGGCACA/ CGTGCTTTGTGATCTGCCGGGT | |
| gRNA oligonucleotide/crRNA sequence | sgRNA | CACCGAAGCTACACTTACTCCAGT/ aaacACTGGAGTAAGTGTAGCTTC | |
| Genomic target sequence(s) | NC_000001.11 [43736346–43736368] | GAAGCTACACTTACTCCAGTGGG | |
| Top off-target mutagenesis predicted site sequencing primers | OT1 | ACATCCACCACTTCTGCTCAT/ACCTACGTAGCGTGATGACT | |
| | OT2 | TCCTTGTGCTGAATGCCTGACC/ ACTTCCAGTCTTGCAAGCTCCA | |
| | OT3 | AATTCCACCGTCCACTGGCTGC/ AATGGGCCAGGAGAGCTGGGTA | |
| | OT4 | TTGGAAGCTGGTTCATCCCA/ATTAGGGCAACCGATGCTGT | |
| | OT5 | AAACGTCTTTGTGGTCCGGGGC/ GGTGGCACTTTAGCTGCTGGCA | |
| ODNs/plasmids/RNA templates used as templates for HDR-mediated site-directed mutagenesis. | N/A | N/A | |
| Backbone modifications in utilized ODNS have to be noted using standard nomenclature. | | | |

*ST3GAL3* inactivation (Table 1). The ST3GAL3-deficient line was generated from the human iPSC line UKWMPi002-A using CRISPR/Cas9. The CRISPR-guide RNA targeted exon 2, containing the start of the open reading frame (Fig. 1A), where insertions or deletions of nucleotides lead to a frameshift of the ST3GAL3 translation. The guide was inserted into the plasmid vector PX459 (Addgene #62988) and transfected into the hiPSCs via nucleofection. After Puromycin selection and single-cell expansion, we performed DNA extraction and PCR cloning to isolate single alleles. Genomic sequencing identified the *ST3GAL3* null mutant (*ST3GAL3-/-*) iPSC line, carrying a deletion of 11 nucleotides in one allele and a deletion of 13 nucleotides in the other (Fig. 1B).

To confirm *ST3GAL3* inactivation at the transcriptomic level, we performed PCR and sequenced the cDNA of the iPSC line (Fig. 1C and Supplementary data). PCR targeting the altered region, specifically expanding the transcriptomic region between exons 2–10, revealed the inability of the line to produce a wild-type transcript for *ST3GAL3* (Fig. 1C, bottom). A second PCR expanding exons 1–3 revealed the production of an abnormal transcript, suggesting the transcription of the longer version of Exon 2, generally absent in wild type lines (Fig. 1C, top). cDNA sequencing corroborated this hypothesis and further confirmed both deletions to be maintained at the transcriptomic level, leading to translational frameshifts and premature stop codon occurrence (Supplementary data).

The line displayed typical pluripotent stem cell morphology. Quantitatively, the pluripotent capacity of the generated line was confirmed via qRT-PCR detection of the markers *NANOG*, *REX1*, and OCT-3/4 (Fig. 1D), and qualitatively, via immunofluorescence staining of TRA1-60, OCT-3/4, and SSEA-4 (Fig. 1E).

The iPSC line was differentiated into all three germ layers to characterize its differentiation potential as confirmed by the expression of the germ-layers markers FOXA2 (endoderm), CD-144 (mesoderm), and PAX-6 (ectoderm) (Fig. 1F).

Karyotype analysis revealed neither structural nor numerical chromosomal abnormalities (Fig. 1H). No unwanted mutations were present in the top 5 off-target sites predicted, as shown by sequencing (Fig. S2). The absence of Sendai virus-related transcripts was confirmed using RT-PCR (Supplementary Fig. S1A). Short Tandem Repeat (STR) analysis demonstrated the identity of all 16 tested loci between the paternal line (UKWMPi002-A) and the generated *ST3GAL3-/-* line (UKWMPi002-A-3). Random plasmid integration was excluded using PCR (Fig. S1B). The line tested mycoplasma-free (Fig. S1C).

## 4. Materials and methods

### 4.1. Cell maintenance

iPSCs were cultured on Matrigel (Corning) coated plates and maintained in StemMACS™ iPSC-Brew medium (Miltenyi) in a humidified atmosphere at 37 °C and 5 % CO2. The medium was changed daily, and cells were passaged with Accutase (Gibco) at approximately 80 % confluency. After passaging, cells were plated in iPSC-Brew medium supplemented with 10 μM ROCK inhibitor (Miltenyi).

### 4.2. CRISPR/Cas9 genomic editing

The sgRNA was designed using Benchling (https://www.benchling.com) and ligated within the pSpCas9(BB)-2A-Puro plasmid V2.0 (PX459; Addgene #62988). 8 x$10^5$ iPSCs were nucleofected with 5 μg of the vector using the Nucleofector™ System (LONZA) and screened with Puromycin (0.7 μg/ml; Invitrogen) exposure for 48 h. Surviving colonies were manually picked and grown in iPSC-Brew medium for three weeks before collecting for DNA and RNA extraction.

### 4.3. Genotyping and sequencing

Genomic DNA from iPSCs and donor cells was extracted using the PureLink™ Genomic DNA Kit (Invitrogen, Thermo Fisher Scientific). Regions of interest were amplified by PCR and products were purified using the NucleoSpin Gel and PCR Clean-up Kit (Macherey-Nagel). Samples carrying biallelic mutations were isolated using a PCR Cloning Kit (NEB) and subsequently sequenced (LGC genomics).

### 4.4. qRT-PCR analysis

Total RNA was extracted using the RNeasy Plus Mini Kit (Qiagen) and reverse-transcribed using the iScript™ cDNA Synthesis Kit (Bio-Rad). cDNA samples were prepared with SYBR™ Select Master Mix (Thermofisher). qRT-PCR was performed using the CFX384 Real-Time System (Bio-Rad). Primers are shown in Table 2.

### 4.5. Germ layer differentiation

Using the StemMACS™ Trilineage differentiation kit (Miltenyi), iPSC lines were differentiated into the three embryonal germ layers, i.e., mesoderm, endoderm, or ectoderm, on Matrigel-coated 6-well plates at a density of 3, 5, or 4 × $10^5$ cells per well, respectively. On day 7, all lines were fixed and tested for specific germ layer markers by immunofluorescence or collected for RNA extraction.

### 4.6. Immunocytochemistry

Cells were fixed with 4 % paraformaldehyde (Roth), blocked (5 % FBS and 1 % BSA in PBS), and permeabilized with 0.2 % Triton X-100 (intracellular markers; Sigma-Aldrich) for 30 min at room temperature (RT). Primary and secondary antibodies (Table 2) and DAPI (300 nM; Sigma-Aldrich) were incubated for 12 h at 4 °C and 1 h at RT, respectively. Cells were visualized under an inverted fluorescence microscope (Olympus).

### 4.7. Karyotype analysis

Karyotypes were verified by GTG-Banding with a resolution of 450 bands in the haploid chromosome set using an Axioskop microscope (Zeiss). In total, eight metaphases were evaluated for numerical abnormalities, six of which were examined further to exclude structural abnormalities.

### 4.8. STR analysis

Genomic DNA from the *ST3GAL3-/-* and paternal lines was isolated using the PureLink™ Genomic DNA Kit (Invitrogen). STR analysis was conducted by Eurofins Genomics via PCR single-locus technology. A total of 16 independent PCR systems, i.e., D8S1179, D21S11, D7S820, CSF1PO, D3S1358, TH01, D13S317, D16S539, D2S1338, AMEL, D5S818, FGA, D19S433, vWA, TPOX, and D18S51 were assessed. Positive and negative controls carried out in parallel yielded correct results.

### 4.9. Mycoplasma test

The supernatant of iPSCs was collected and processed using the LookOut® Mycoplasma PCR Detection Kit (Sigma-Aldrich) to exclude mycoplasma contamination.

## Declaration of Competing Interest

The authors declare that they have no known competing financial interests or personal relationships that could have appeared to influence the work reported in this paper.

## Acknowledgments

This work was supported by ERA-NET NEURON under Grant No. 01EW1902 (DECODE!), the Horizon 2020 Research and Innovation Programme under Grant No. 728018 (Eat2beNICE), Grant No. 953327 (Serotonin and Beyond), the Horizon Europe Research and Innovation Programme under Grant No. EU 101086453 (Aqua-Synapse), the DFG (Grant No. 413657723, Clinician Scientist-Program UNION CVD), and the University of Würzburg in the funding program Open Access Publishing. We thank Julia Merk, Gabriela Ortega, and Nicole Schraud for excellent technical assistance.

## Appendix A. Supplementary data

Supplementary data to this article can be found online at https://doi.org/10.1016/j.scr.2023.103038.

## References

Demontis, D., Walters, R.K., Martin, J., Mattheisen, M., Als, T.D., Agerbo, E., Baldursson, G., Belliveau, R., Bybjerg-Grauholm, J., Bækvad-Hansen, M., et al., 2019. Discovery of the first genome-wide significant risk loci for attention deficit/hyperactivity disorder. Nat. Genet. 51 (1), 63–75.

Hu, H., Eggers, K., Chen, W., Garshasbi, M., Motazacker, M.M., Wrogemann, K., Kahrizi, K., Tzschach, A., Hosseini, M., Bahman, I., Hucho, T., Mühlenhoff, M., Gerardy-Schahn, R., Najmabadi, H., Ropers, H.H., Kuss, A., 2011. ST3GAL3 mutations impair the development of higher cognitive functions. Am. J. Hum. Genet. 89 (3), 407–414.

Indellicato, R., Domenighini, R., Malagolini, N., Cereda, A., Mamoli, D., Pezzani, L., Iascone, M., dall'Olio, F., & Trinchera, M. (2020). A novel nonsense and inactivating variant of ST3GAL3 in two infant siblings suffering severe epilepsy and expressing circulating CA19.9. Glycobiology, 30(2), 95-104.

Rivero, O., Alhama-Riba, J., Ku, H.-P., Fischer, M., Ortega, G., Álmos, P., Diouf, D., van den Hove, D., Lesch, K.P., 2021. Haploinsufficiency of the attention-deficit/hyperactivity disorder risk gene St3gal3 in mice causes alterations in cognition and expression of genes involved in myelination and sialylation. Front. Genet. 12, 688488.

Schnaar, R.L., Gerardy-Schahn, R., Hildebrandt, H., 2014. Sialic acids in the brain: gangliosides and polysialic acid in nervous system development, stability, disease, and regeneration. Physiol. Rev. 94 (2), 461–518.